

1 *Original Article Submission to the ICES Journal of Marine Science*

2

3 Incorporating spatiotemporal variability in multispecies survey design optimization addresses
4 tradeoffs in uncertainty

5

6 Zack S. Oyafuso*, Lewis A.K. Barnett, Stan Kotwicki

7

8 National Marine Fisheries Service

9 Alaska Fisheries Science Center

10 National Oceanic and Atmospheric Administration

11 7600 Sand Point Way NE

12 Seattle, WA 98115

13

14 *corresponding author: Zack S. Oyafuso

15 Email: zack.oyafuso@noaa.gov

16 Office Phone Number: (206) 526-4083

17

18 Keywords: Survey Optimization; Gulf of Alaska; Bottom-Trawl Survey; Stratified Random
19 Sampling; Genetic Algorithm;

20

21

22

23

24 **Abstract**

25 In designing and performing surveys of animal abundance, monitoring programs often struggle
26 to determine the sampling intensity and design required to achieve their objectives, and this
27 problem greatly increases in complexity for multispecies surveys with inherent tradeoffs among
28 species. To address these issues, we conducted a multispecies stratified random survey design
29 optimization using a spatiotemporal operating model and a genetic algorithm that optimizes both
30 the stratification (defined by depth and longitude) and the minimum optimal allocation of
31 samples across strata subject to prespecified precision limits. Surveys were then simulated under
32 those optimized designs and performance was evaluated by calculating the precision and
33 accuracy of a resulting design-based abundance index. We applied this framework to a
34 multispecies fishery-independent bottom trawl survey in the Gulf of Alaska, USA. Incorporating
35 only spatial variation in the optimization failed to produce population estimates within the
36 prespecified precision constraints, whereas including additional spatiotemporal variation ensured
37 that estimates were both unbiased and within prespecified precision constraints. In general,
38 results were not sensitive to the number of strata in the optimized solutions. This optimization
39 approach provides an objective quantitative framework for designing new, or improving existing,
40 survey designs for many different ecosystems.

41

42

43

44

45

46

47 **1. Introduction**

48 Productive and sustainable fisheries provide socioeconomic opportunities and ensure food and
49 nutritional security. In the United States, commercial wild-capture fisheries totaled 4.3 million
50 metric tons valued at \$5.6 billion in 2018 (NMFS, 2020). Fisheries stock assessments provide the
51 basis for managing these fisheries. Fishery-independent surveys are often the primary source of
52 inputs for stock assessment models, providing information on the abundance and composition of
53 fish populations. Thus, properly designed fisheries surveys are integral to ensuring that the most
54 scientifically robust data products are used for fisheries management (Smith and Hubley, 2014;
55 Zimmermann and Enberg 2016; Muradian et al. 2019). Survey data are also used to address a
56 variety of research questions including species distributions over time (e.g., Thorson et al.,
57 2015), ecosystem status indicators through environmental data collection (e.g., de Boois, 2019;
58 Zador et al., 2019).

59
60 Accuracy and precision are the main quality metrics of a fisheries survey and are constrained by
61 total sampling effort and budget. The precision of a survey, described as either a variance or a
62 coefficient of variation (CV) is an important survey output commonly used for survey
63 comparison studies (Overholtz et al., 2006), evaluations of survey outputs quality (Cao et al.,
64 2014), and stock assessments (Francis, 2011). That said, fisheries surveys need to be flexible to
65 many sources of logistical constraints and uncertainties while still maximizing the objectives of
66 producing survey products with high accuracy and precision. Unavoidable survey effort
67 reduction due to budgetary constraints, inclement weather, or vessel breakdowns pose serious
68 implications to the reliability of fisheries surveys (ICES, 2020). Reductions in survey effort
69 through a reduction in sampling intensity or frequency can compromise the precision and bias of

70 abundance indices (ICES, 2020; Hutniczak et al., 2019; von Szalay, 2015). Additionally, fishery-
71 specific constraints like gear type, coverage rate, and vessel type are other additional
72 considerations when optimizing survey design (Miller et al., 2006). Given the high operating
73 costs of fisheries-independent surveys and that these changes typically occur at time scales that
74 leave little time for planning and quantitative evaluation, there is a need for rapid survey
75 optimization tools to guide survey changes within a flexible framework.

76
77 The multispecies nature of many surveys means that invariably there are interspecific tradeoffs
78 in designing a survey that optimizes over many species (and possibly life stages within species)
79 with different spatiotemporal distributions and varying levels of directed targeting (Wang et al.,
80 2018; Smith et al., 2011). The magnitude of variance in species abundance across space and/or
81 time affects the optimal spatial extent and frequency of surveys (Lanthier et al., 2013; Rhodes
82 and Jonzén, 2011). In some cases, there may be temporary needs for increased precision for
83 certain species and/or regions (e.g., when a stock is close to a limit threshold or displays sudden
84 declines in abundance; Laurel and Rogers, 2020; Barbeaux et al., 2017). Further, tradeoffs in
85 survey design strategies can occur among data uses e.g., indices of abundance, compositional
86 data, species distribution shifts, and population responses to marine reserve implementation
87 (Smith et al. 2011; Miller et al., 2006). Thus, the evaluation of the effects of changes in total
88 survey effort needs to also consider tradeoffs of quality metrics among species.

89
90 To illustrate the development of a fishery survey design optimization framework while
91 addressing the above challenges related to survey effort reduction and tradeoffs among species,
92 we focused on a case study involving the Gulf of Alaska (GoA) groundfish stratified random

93 bottom-trawl survey (BTS). With a relatively long time series (nearly 40 yr in this case) of data
94 on the distribution of these species, both spatiotemporal variability and/or species covariation
95 can be incorporated into a more goal-driven and objective survey design optimization (e.g., Peel
96 et al., 2012). The stratified survey optimization was conducted using a genetic algorithm that
97 optimizes both the stratification of the spatial domain as to minimize total sample size subject to
98 prespecified precision constraints for a given number of strata. We used a previously built
99 multispecies spatiotemporal fish density distribution model as data inputs to the optimization.
100 Surveys were then simulated under those optimized survey designs and the precision and bias of
101 the population estimates were calculated as performance metrics. This framework for optimizing
102 a stratified random survey design for estimating abundance with respect to a model-generated
103 spatiotemporal distribution can be used to evaluate the multispecies tradeoffs of varying
104 sampling intensities on the quality of fisheries survey estimates.

105

106 **2. Methods**

107 The framework of the optimization is presented in Figure 1. Section 2.1 is a brief overview of the
108 multispecies spatiotemporal operating model, from which predicted densities are used as data
109 inputs to the survey optimization algorithm. The optimization problem is defined in Section 2.2
110 and the algorithm used to solve the optimization problem is described in Section 2.3. Section 2.4
111 describes how the survey optimization is conducted in the GoA and 2.5 describes the simulation
112 of those optimized survey designs against the operating model and the resulting performance
113 metrics. The associated code can be found on the corresponding author's GitHub page
114 (https://github.com/zoyafuso-NOAA/Optimal_Allocation_GoA_Manuscript).

115

116 Three types of CVs are defined in the following sections with slightly different interpretations
117 and uses in this framework. In sections 2.2-2.4, CVs that incorporate variability in density across
118 the domain and observed years for each species from the operating model described in section
119 2.1 and are used as prespecified constraints of precision to guide the optimization of a new
120 multispecies stratified survey design. These CVs utilize population-level stratum variance
121 statistics that integrate the many sources of process variability as specified in the OM in Section
122 2.1 with the exception of additional sources of measurement error. These CV constraints can be
123 interpreted as the expectation of the sample CV for a given level of survey effort. The survey
124 simulation in Section 2.5 is important in establishing precision levels more consistent with what
125 would be observed in the sampling process. Within a simulation framework, the second CV
126 defined in 2.5 describes the variability of an abundance index across many simulated surveys
127 relative to the the true index, interpreted as the realized or “true” sampling CV (Kotwicki and
128 Ono, 2019), a metric impossible to calculate when analyzing actual surveys. The sample CV is
129 the third type of CV used in this analysis and refers to the CV associated with the abundance
130 index calculated for one replicate survey. Unlike the CV constraints, these CV utilize sample-
131 level statistics of stratum variance and are year-specific. The congruence of these sample CVs to
132 the realized true CV is a performance metric defined in Section 2.5.

133

134 2.1 Operating Model

135 To serve as an operating model, we fitted a multispecies spatiotemporal distribution model to
136 catch rate data using a vector-autoregressive spatiotemporal model (VAST; Thorson and Barnett,
137 2017). Readers are referred to the Supplementary S1 for more detail on the VAST operating
138 model, but a brief description of the relevant outputs follows. We fitted the VAST model to

139 catch-per-unit-effort data of GoA groundfishes collected from a fishery-independent BTS using a
140 stratified random sampling design (von Szalay and Raring, 2018). We restricted the input data to
141 the years 1996, 1999, and every other year from 2003 to 2019 to ensure consistency in
142 sampling design and species identification (11 observed data years). Fourteen species and one
143 species group were included to represent the groundfish complex in the GoA, based on
144 commercial value and the dependence of stock assessment models on survey-derived abundance
145 indices: *Atheresthes stomias*, *Gadus chalcogrammus*, *G. macrocephalus*, *Glyptocephalus*
146 *zachirus*, *Hippoglossoides elassodon*, *Hippoglossus stenolepis*, *Lepidopsetta bilineata*, *L.*
147 *polyxystra*, *Limanda aspera*, *Microstomus pacificus*, *Sebastes alutus*, *S. polyspinis*, *S. variabilis*,
148 and *Sebastolobus alascanus*. Due to identification issues between two rockfishes, *Sebastes*
149 *melanostictus* and *S. aleutianus*, the catches of these two species were combined into a species
150 group (*Sebastes* spp.) we will refer to as “*Sebastes* B_R” (blackspotted rockfish and rougheye
151 rockfish, respectively) hereafter.

152

153 The density (y_{git}) of each species or species group was predicted onto the GoA survey spatial
154 domain at a resolution of 3.7 by 3.7 km ($i: 1, 2, \dots, N = 23\,339$ cells; some prediction grid cells
155 had smaller area due to intersections with survey domain boundaries) for each species
156 ($g: 1, 2, \dots, G = 15$ species) and observed year ($t: 1, 2, \dots, T = 11$ observed years). Figure 2
157 shows the average spatial distribution over time for each species. These predictions were
158 taken to represent “true” densities values, which were used to generate optimal survey
159 designs and evaluate the performance of simulated surveys given those designs. As the primary
160 measure of survey performance is the accuracy and precision of the total abundance estimate, we
161 define this by the proxy of mean density.

162

163 2.2 Survey Optimization Problem

164 The goal of the multispecies stratified survey design optimization is to jointly optimize the
165 stratification and the sample allocation across strata ($h: 1, 2, \dots H$) by finding that which
166 minimizes total sample size, subject to prespecified precision constraints for each species.

167 Specifically, the objective function is to minimize total sample size subject to G prespecified
168 coefficient of variation (CV) constraints (U_1, U_2, \dots, U_G):

169
$$\min \sum_{h=1}^H n_h \quad \text{[Equation 1]}$$

170
$$\begin{aligned} & s. t. \\ & CV(Y_1) < U_1 \\ & \dots \quad \text{[Equation Set 2]} \end{aligned}$$

173
$$CV(Y_G) < U_G ,$$

174
$$CV(Y_g) = \frac{\sqrt{Var(Y_g)}}{Y_g} \quad \text{[Equation 3]}$$

175
$$Var(Y_g) = \sum_{h=1}^H \left(\frac{N_h}{N}\right)^2 \frac{S_{h,g}^2}{n_h} \left(1 - \frac{n_h}{N_h}\right) \quad \text{[Equation 4]}$$

176 where n_h and N_h are the sample sizes and number of sampling units in stratum h , respectively.

177 By leveraging density predictions provided by the OM, this optimization is specified using

178 population-level statistics. Y_g is the population mean of species g averaged over the cells in the

179 spatial domain and over observed years. $Var(Y_g)$ in Equation 4 is the stratified random sampling

180 variance associated with the population mean. Careful consideration is needed for this variance,

181 specifically the stratum variance $S_{h,g}^2$, defined in Equation 4. The OM provides predicted

182 densities across all cells and observed years for each species and integrates many sources of

183 variation including temporal (year-to-year), habitat covariates (depth), species covariation, and

184 additional spatial and spatiotemporal variation. A common issue in survey design optimization is

185 how to integrate data from previous surveys (Francis, 2006), thus we investigated two types of
186 stratum variances that incorporated the OM-derived densities predicted across the observed
187 survey years in the GoA BTS:

188

189 1) Spatial-only stratum variance: The first method was to reduce the temporal dimension by
190 averaging the predicted densities from the OM over the observed years for each cell in the spatial
191 domain. In this “spatial-only” optimization, $S_{h,g}^2$ is the population stratum variance of density for
192 species g in stratum h :

$$193 \quad S_{h,g}^2 = \frac{1}{N_h - 1} \sum_{i=1}^{N_h} (\overline{y_{gi}} - \overline{y_{hg}})^2, [Equation 5]$$

194

195 where $\overline{y_{hg}}$ is the population mean density estimate of species g averaged across all observed
196 years and cells contained within stratum h , and y_{gi} is the predicted density of species g in cell i
197 (where cell i is in stratum h) averaged across observed years. Note the use of the N_h term in
198 Equation 5 denotes a population-level stratum variance.

199

200 2) Spatiotemporal stratum variance: A potential issue with the spatial-only version of the
201 population stratum variance is underestimating the total “known” variability within a stratum by
202 averaging over the year-to-year as well as spatiotemporal variation explicitly modeled in the
203 OM. Thus, for this “spatiotemporal” optimization, the population-level stratum variance in
204 Equation 5 was modified to incorporate both within-stratum (note the summation range between
205 $i = 1$ to N_h) density variation and within-grid cell densities variation across years (note the
206 summation range between $t = 1$ and T):

$$207 \quad S_{hg}^2 = \frac{1}{TN_h - 1} \sum_{t=1}^T \sum_{i=1}^{N_h} (y_{git} - \overline{y_{hg}})^2 [Equation 6]$$

208

209 2.3 Optimization of Strata Boundaries and Sample Allocation

210 Comprehensive brute-force searches for the optimum stratification of the spatial domain and
211 optimum allocation of samples are usually intractable for moderately sized problems. Thus, we
212 searched for optimal stratifications and survey effort allocations via a genetic algorithm using the
213 R package `SamplingStrata` (Barcaroli, 2014; Ballin and Barcaroli, 2013) . The genetic
214 algorithm uses evolutionary principles such as fitness-based selection, recombination, and
215 mutation to iteratively search for an optimal stratification and sample allocation. Below, we
216 provide a brief description of the algorithm and settings used but readers are referred to Ballin
217 and Barcaroli (2013) for more technical details.

218

219 The optimization initializes with 30 random stratifications (a prespecified number of candidate
220 solutions) based on two auxiliary variables, bottom depth (m) and longitude (eastings, km) for a
221 user-defined number of strata. Here, we explore results from 5 to 60 strata to determine how the
222 number of strata influences the precision of the abundance estimate. In the GoA, gradients across
223 both depth and location have been observed to describe major patterns in demersal species
224 composition (Mueter and Norcross, 2002). Longitude was used as a one-dimensional east-west
225 location proxy. For each candidate solution, the Bethel algorithm (Bethel, 1989) is used to
226 optimize the allocation of the minimum sample size across strata, subject to equations 1-2.
227 Fitness is defined as the resultant sample size from the Bethel algorithm, with solutions with
228 lower sample sizes having higher fitness. Elitism occurs by taking the solutions with highest
229 fitness (defined *a priori* to be solutions in the top 10th percentile for smallest sample size) and
230 automatically advancing them to the next iteration of the algorithm. In the next iteration the

231 remaining solutions are selected with probability proportional to their fitness values to
232 “procreate” a new solution by applying a crossover of the solutions. Random changes in the
233 stratifications, or mutations, are then applied at a given rate to the resultant solution. The
234 mutation rate defines how often random changes to the solutions occur and was tuned to $1/(1 +$
235 $H)$ based on previous tuning guidelines (G. Barcaroli, personal communication) to reach
236 reasonable convergence times. The process of procreation occurs until 30 candidate solutions are
237 included in the next iteration of the algorithm. The algorithm is conducted for a total of 200
238 iterations, a value (along with the choice of 30 candidate solutions) chosen to ensure that, at least
239 qualitatively, the algorithm reached an asymptotically optimal solution within a reasonable
240 amount of computation time (see Supplementary S3 for an example of the algorithm output).

241

242 2.4 Optimization Schemes

243 In the GoA, total sampling effort is primarily determined by how many boats are available to
244 conduct the survey, with all vessels operating for the same duration of time. These levels of
245 sampling intensity correspond to approximately: 280 samples (1 boat), 550 (2 boats) and 820 (3
246 boats) (von Szalay and Raring, 2018; von Szalay et al., 2010). Thus, we focused on optimized
247 survey designs under these three sample size scenarios for a given number of strata. The
248 optimization does not maximize precision constrained by a total sample size, thus we needed
249 to set the CV constraints (Equation Set 2) for each species to meet the three sample size
250 scenarios regardless of which version of the stratum variance (spatial-only or spatiotemporal,
251 Equations 5 or 6, respectively) is used. We implemented this systematically using two sets of
252 rules depending on whether the CV constraint was constant or varying among species:

253 1) One-CV constraint scenario: CV constraints were set to the same value across species.
254 Initially the CV constraint was set to some arbitrarily high value (e.g., 0.30) and the
255 optimization was conducted to produce the optimal stratification and total sample size.
256 Then, the population CV constraint is incrementally decreased (e.g., 0.30 to 0.29) and the
257 optimization was conducted again. By gradually decreasing the CV constraint, the
258 optimized sample size slowly increases. This increment was chosen to be small enough to
259 balance having adequate coverage over the three boat-effort scenarios ($n = 280, 550, 820$
260 stations) within a reasonable total computation time. This process was iterated until the
261 range of considered sample sizes was captured (i.e., until the optimized sample size was
262 ≥ 820).

263 2) Species-specific CV constraint scenario: CV constraints were allowed to differ across
264 species. Similar to the one-CV constraint scenario, the CV constraint was initialized to be
265 the same across species at some arbitrarily high value (e.g., 0.30). The optimization was
266 conducted, and the optimized CVs across species (i.e., $CV(Y_1), CV(Y_2), \dots, CV(Y_G)$) were
267 saved from the optimization. The CV constraints for the next instantiation were
268 calculated by reducing the optimized CVs in the previous run by some proportional
269 increment (e.g., 5%) for each species. Similar to the one-CV method, this process was
270 iterated until the range of the three boat-effort scenarios was captured.

271

272 2.5 Simulation of data collection

273 For each combination of strata number and sample size scenario, the optimized survey was
274 simulated $D = 1000$ times. r_{dgt} is the stratified random sample estimate of mean density of
275 species g at time t for simulated survey d . $CV(r_{dgt})$ is the CV of the survey estimate and is

276 similar to Equations 3-4 except using the sample stratum variance instead of the population
 277 stratum variance. To evaluate the precision and accuracy of the abundance estimates resulting
 278 from simulated surveys, we calculated the following performance metrics for each species.

279

280 Since our procedure does not optimize sample CVs directly, we evaluated the expected effect of
 281 a survey optimized with respect to population CVs on performance metrics of the sample CVs
 282 derived from simulated surveys. The “true” CV, $CV_{TRUE}(Y_{gt})$, describes the precision of the
 283 mean density estimate of species g at time t across replicate surveys and is the standard deviation
 284 of the simulated survey estimates (where \bar{r}_{gt} is the mean density estimate of species g at time t
 285 averaged across the D surveys) relative to r_{gt} , the true mean density of species g at time t :

$$286 \quad CV_{TRUE}(Y_{gt}) = \frac{\sqrt{(D-1)^{-1} \sum_{d=1}^D (r_{dgt} - \bar{r}_{gt})^2}}{Y_{gt}}. \text{ [Equation 7]}$$

287 Relative root mean square error of CV, $RRMSE(CV(r_{dgt}))$, is a measure of uncertainty of the
 288 replicate sample CVs of species g at time t and is a composite measure of the dispersion and bias
 289 of the replicate sample CVs about the true CV:

$$290 \quad RRMSE(CV(r_{dgt})) = \frac{\sqrt{D^{-1} \sum_{d=1}^D (CV(r_{dgt}) - CV_{TRUE}(Y_{gt}))^2}}{D^{-1} \sum_{d=1}^D CV(r_{dgt})}. \text{ [Equation 8]}$$

291

292 Lastly, relative biases (RB) of the mean density and CV estimates relative to their respective true
 293 values were calculated as

$$294 \quad RB(r_{dgt}) = 100\% \frac{\sum_{d=1}^D (r_{dgt} - Y_{gt})}{D Y_{gt}} \text{ [Equation 9]}$$

295

$$296 \quad RB(CV(r_{dgt})) = 100\% \frac{\sum_{d=1}^D (CV(r_{dgt}) - CV_{TRUE}(Y_{gt}))}{D CV_{TRUE}(Y_{gt})} \text{ [Equation 10]}$$

297

298 **3. Results**

299 3.1 Optimal stratification : The optimization solutions with the closest sample sizes to each of
300 the three intended sample sizes were chosen as the representative solutions. Figure 3 shows those
301 three representative solutions along with examples of simulated survey stations for five, ten, and
302 fifteen strata. The longitudinal variable was generally cut into the west, central, and eastern parts
303 of the spatial domain. Strata in the eastern part of the domain were often connected with the
304 deeper continental slope strata. Sampling density was concentrated in the western and central
305 parts of the spatial domain, with sparse sampling in the eastern portion. Solutions across boat-
306 effort scenarios within a strata number scenario were generally consistent in the strata
307 boundaries.

308

309 3.2 Tradeoff between sample size and CV constraint: The spatial-only optimization led to one,
310 two, and three boat solutions with expected CV constraints of 0.19, 0.13, and 0.10, respectively
311 (Figure 4). These CV constraints are from the one-CV constraint approach, meaning these values
312 represent the maximum expected sampling CV that any one species can exhibit. The addition of
313 spatiotemporal variability of the optimization increased the CV constraints across boat-effort
314 scenarios to 0.28, 0.21, and 0.17, respectively. For a given CV constraint, the addition of
315 spatiotemporal variability required roughly 2-3 \times more samples in the optimal solution. Figure 4
316 shows the relationship between sample size and CV for a five-strata scenario only, but this
317 pattern was consistent across scenarios with different numbers of strata (Supplementary S4).

318

319 3.3. Expected vs realized precision: True CV encompasses the variability of the mean density
320 estimates across realized survey replicates relative to the true mean density and is different from

321 the prespecified (expected) CV constraints used to constrain the survey optimization algorithm.
322 Simulation testing allows for the evaluation of the congruency of the true CV across years to the
323 CV constraint. Simulated surveys under the spatial-only optimization failed to produce true CVs
324 lower than the CV constraint consistent across observed years for some species (Figure 5). The
325 median of the distribution of true CV across years for *Sebastes alutus*, *S. polyspinis*, and *S.*
326 *variabilis* were 25-50% higher than the CV constraints specified in the optimization. When
327 spatiotemporal variability was included in the optimization, all species were surveyed with true
328 CVs lower than the CV constraints for the majority, if not all, years observed. Further, under the
329 species-specific CV constraint scenario, all species were surveyed with true CVs at or slightly
330 below their respective CV constraints. Additionally, the medians of the distributions of the true
331 CVs were much closer to the expected CV than the one-CV constraint scenarios. These patterns
332 were consistent across scenarios with different numbers of strata (Supplementary S5).

333
334 3.4 True CV across strata and sample sizes: Increasing sampling intensity reduced the true CV
335 and the spread of the bias of the mean density estimate across species and strata scenarios
336 (Figures 6-7). Estimates of mean density across species showed low bias (Figure 7), with slightly
337 negative median biases up to 5%. Increased samples across species led to further reductions in
338 bias and there were no noticeable differences in this effect across number of strata. There were
339 also no noticeable trends in true CV across number of strata for either the one-CV constraint
340 (Supplementary S6) or species-specific CV constraint optimizations (Figure 7).

341
342 3.5 Relative Root Mean Square Error of CV across strata and sample sizes: The RRMSE of CV
343 encompasses both the bias and variability of the simulated sample CVs about the true CV.

344 Similar to true CV, increasing sampling reduced the uncertainty and spread of the bias of the
345 sample CV estimates across species and strata scenarios with high consistency between both
346 optimization types (Figures 8-9). An exception was the RRMSE of CV being higher for larger
347 numbers of strata for a handful of species (e.g., slope-dwellers such as *Sebastes B_R* and
348 *Sebastolobus alascanus*) for the one-CV constraint optimization (Figure 8). There was less of a
349 noticeable trend across strata in RRMSE of CV for the species-specific CV constraint
350 optimization than for the one-CV constraint optimization (Supplementary S7). The species-
351 specific CV constraint optimization was more consistent in demonstrating the pattern of lower
352 true CV and RRMSE of CV with increasing sample sizes, particularly with *M. pacificus*,
353 *Sebastolobus alascanus*, *Sebastes B_R*, *L. bilineata*, and *L. polyxystra*. Simulated sample CVs
354 were slightly negatively biased relative to their respective true CV value with smaller magnitude
355 and variability with increasing sampling intensity (Figure 9), regardless of the CV-constraint
356 approach used.

357

358 **4. Discussion**

359 The inclusion of spatiotemporal variability in the population stratum variance calculation
360 (Equation 6) led to CV constraints that were within the distribution of the true or realized CVs of
361 abundance when surveys were simulated. These CV constraints are equivalent to those the user
362 defines initially in Equation Set 2, thus the main goal of the survey simulation was the evaluate
363 the congruency between the expected CV constraints and realized CVs in the form of the true
364 CVs. In contrast, CV constraints using the spatial-only version of the population stratum
365 variance (Equation 5) were not consistent with true CVs across species, with true CVs for some
366 of the more variable *Sebastes* species vastly underestimated. The issue of including historical

367 variation in the survey data has been discussed in detail previously (Francis, 2006), one
368 complication being that incorporating year-to-year variation in our operating model may
369 overestimate the within-stratum variability. In fact, the tradeoff of adding spatiotemporal
370 variation to the stratum variance calculation (Equation 6) was a 2-3 \times increase in sample size for
371 a given CV constraint (Figure 4), with many species' distributions of true CV lower than their
372 respective CV constraints (Figure 5). However, the consistency between the true CVs and
373 their respective CV constraints across species and years supports the use of this optimization to
374 provide robust and consistent indices of abundance. Furthermore, future applications of this
375 approach should also integrate within the optimization framework other important sources of
376 observation error not included in this analysis, e.g., measurement error, untrawlable areas,
377 detectability (Field et al., 2005), and sampling efficiency (Kotwicky and Ono, 2019), especially
378 when realistically simulating surveys and assessing performance. The exclusion of additional
379 sampling error in our framework limits the absolute interpretability of the CV constraints and true
380 CVs, thus these CVs could be treated as the "best case" or lower limits of expected
381 sampling CVs.

382
383 Specifying precision constraints for each species is a clear advantage of this survey optimization
384 framework and allows increased flexibility for survey planners to meet desired goals in their
385 survey designs. When we initially used the one-CV constraint method to solve the optimization
386 problem, there were some inconsistencies in simulated true CV (Supplementary S6) and
387 RRMSE of CV (Figure 8) and sampling intensity for some species. With the one-CV constraint
388 approach, a single CV constraint is defined for all species, thus the CV constraint imposed in
389 the optimization is strict for some species and less so for others, which can produce these

390 inconsistent findings. The species-specific CV constraint approach seemed to produce more
391 consistent positive trends in the performance metrics with increasing sampling intensity by
392 defining CV constraints for each species individually. By setting constraints for each species
393 specifically and allowing the CV constraints to reduce proportionally for each species ,
394 solutions performed more consistently with increasing sampling intensity. Setting CV constraints
395 for each species also gives survey planners more flexibility to emphasize or de-emphasize certain
396 species within the optimization more explicitly while evaluating the resulting tradeoffs in
397 precision for the other species. The CV constraint utilized in this optimization was a
398 maximum constraint but additionally, minimum CV constraints can be also provided from stock
399 assessment programs to provide additional constraints on the optimization. We naively assumed
400 in the species-specific CV approach that the CV constraints need not be lower than 10%, but
401 these values can be based on different priorities for different species. Work is currently being
402 done for that purpose in the Gulf of Alaska stock assessments (ICES, 2020), based on how
403 sampling precision affects uncertainty of assessment outputs such as estimated biomass.
404 Ultimately, a cost-benefit analysis evaluating the relationship between total sampling effort,
405 precision, and downstream management quantities like total allowable catch can more directly
406 link the multispecies tradeoffs of surveys on the economic value of fisheries (Francis, 2006).

407
408 While there are many approaches to optimizing survey design, the framework introduced
409 provides a new approach to optimize a survey design that is particularly advantageous for
410 estimating animal abundance time series. Previous simulation studies have shown that reductions
411 in precision from lowered sampling can be alleviated by choosing a more optimal stratification
412 scheme (Xu et al., 2015). Peel et al. (2012) developed a survey optimization based on a

413 multispecies model-based (Generalized Additive Model) survey design. With the increasing
414 usage of model-based spatiotemporal methods to develop indices of abundance (Thorson and
415 Barnett, 2017; Thorson et al., 2015, 2017), it is becoming more relevant to develop formalized
416 survey design optimizations in tandem with these model-based estimation methods. Other
417 weighted multiple-criterion optimizations of stratified surveys focused on optimizing over
418 additional data types like compositional and bycatch data (Miller et al., 2006). With emerging
419 OMs like those presented in the SimSurvey R package (Regular et al., 2020), age- and spatially
420 explicit OMs are becoming more accessible to incorporate other data types in a survey
421 optimization.

422

423 The framework that we present can be used as a tool for long-term decision support for
424 improving current surveys and resulting survey data products such as abundance indices and
425 age or size composition estimates. For example, modifying the current stratified survey
426 design in the GoA is a long-term process that will involve rigorous review and operational
427 modifications over multiple years. Fortunately, the switch to a more efficient survey design
428 would not require calibration, as the change would be between two stratified random designs
429 which are inherently unbiased. Work is currently ongoing to compare the performance of this
430 survey design framework versus the current GoA survey design via simulation testing. Currently
431 the GoA BTS survey uses a stratified random design with 59 strata defined by bathymetry,
432 bottom terrain, and statistical reporting designations (von Szalay and Raring, 2018). While
433 upwards of 60 strata are not inherently too many strata, the delineations of the strata boundaries
434 were subjectively chosen during a time where less information was known about the demersal
435 species set. Furthermore, the existence of such numerous strata can cause problems computing

436 sample-level stratum variances, as some strata can become undersampled to the extent that it is
437 impossible to estimate a variance or variances are estimated with uncertainty too high to provide
438 meaningful abundance estimates. From these preliminary results on the GoA survey design, an
439 unbiased survey design can be optimized with less strata than used currently (e.g., 10-20 strata
440 instead of 55-59).

Integral to potentially changing the survey design
441 in the GoA is understanding the current performance and tradeoffs of the present survey design.
442 Metrics such as true CV, relative bias, and RRMSE of CV can be used to show any deficiencies
443 in the current design and how to improve future survey designs and sampling allocations. The
444 uncertainty associated with the sample CVs is related to its reliability as a data weight in some
445 stock assessments (Francis, 2011) but is often overlooked in fisheries science despite such
446 estimates themselves often being highly uncertain (Kotwicki and Ono, 2019). The slight negative
447 bias in the sample CVs relative to the true CV, especially for highly variable species
448 (*Sebastes* spp., Figures 8 and 9), contributed to the magnitude of the RRMSE of CV, and was
449 expected given the patchy nature of these species' distributions. It is key to emphasize temporal
450 variability in both the estimates and their associated uncertainties when evaluating and
451 planning reliable and quality surveys.

452
453 These solutions are intended to objectively guide future survey designs we expect that the
454 actual boundaries of the strata would be further modified based on expert opinion, logistical
455 aspects of the survey operation, or other information sources prior to implementation. For
456 example, the way the optimization partitioned depth and longitude resulted in unnatural
457 longitudinal cuts that split islands, bays, and inlets. If this produces features that do not seem
458 consistent with other data or knowledge of the system, other variables could be used to determine

459 stratification and additional fine-scale habitat features could be incorporated as covariates in the
460 operating model. Post-hoc, the shapes of the strata may also be changed to increase the
461 feasibility and representation of the design. For example, some GoA groundfishes are managed
462 within either three management areas or five management districts that roughly divide the
463 domain into western/central/eastern areas. Work is currently ongoing to evaluate the effects of
464 including these management strata either into the optimization as a separate stratum variable,
465 conducting the optimization separately in each management strata, or through some post-
466 stratification process. Survey teams may also be interested in the average distance among
467 stations produced by optimal allocation, as logistical challenges may prevent certain parts of the
468 spatial domain to be surveyed in a cost-efficient manner. For example in the current GoA BTS
469 survey, one- and two-boat allocations currently do not sample the deepest strata due to time
470 constraints. Survey design optimization packages like the SamplingStrata package (Barcaroli,
471 2014) can also incorporate survey costs with respect to survey duration per station or distance
472 from port or limit the spatial domain to feasible depth ranges and trawlable (i.e., accessible)
473 areas. The advantage of this systematic approach is that these modifications can be evaluated
474 in a reproducible and transparent way to document the survey design process.

475

476 In addition to redesigning the stratification and sample allocation of existing surveys, the
477 framework presented here could also be used to design surveys in new regions, or to optimize
478 survey effort allocation within an existing stratification. However, applying this complete
479 framework to optimize surveys may not always be feasible given the requirement of thorough
480 species distribution modelling efforts to predict population density across the spatial domain at
481 the resolution of the sampling unit. Fortunately, the optimization is a two-step process that first

482 creates stratifications and then applies a multivariable optimal allocation algorithm (Bethel,
483 1989). Thus, in cases where a complete surface of density predictions is not available, the Bethel
484 algorithm can be used on its own to provide optimal effort allocations given pre-specified strata
485 boundaries and historical strata-level sampling means and variances. The framework of
486 specifying CV constraints would be similar to our approach but without the implementation of a
487 genetic algorithm to find optimal strata boundaries. For instance, we could have used the Bethel
488 algorithm on the GoA survey example with the 59 previously defined strata, where data inputs
489 would be the historical sample strata means and variances. This reduced version of the
490 optimization framework could be applied as an intermediary approach, providing the time and
491 additional data needed to complete the species distribution modeling necessary to perform the
492 full optimization. Alternatively, survey planners could opt for one optimized stratified survey
493 and adjust allocations using the Bethel algorithm based on potential future effort levels while
494 making these new strata boundaries constant. We do not explicitly recommend that the
495 stratification be changed between times with different sampling effort. However, if such changes
496 were implemented, the survey time series would still be easily interpretable as we expect all
497 stratified random sampling designs to produce unbiased estimates.

498

499 By leveraging the nearly 25-year time series of survey data, we can both incorporate the
500 observed spatiotemporal variation to inform the design of the survey to meet a desired level of
501 precision and continue to do so as data accrue over time. The updating of information over time
502 reflects a major advantage of a survey design that can improve over time, and this framework is
503 one way to provide an explicit but flexible framework for that process. That said, survey
504 teams often have to contend with environmental changes that may cause species distributions to

505 shift from their previously predicted distributions (e.g., Muhling et al., 2020). Such distribution
506 shifts can influence both the optimality of the previous survey design and more fundamentally
507 bias estimates due to changes in catchability and spatial availability. Survey designs can be
508 flexibly optimized to account for environmental information and then updated based on short-
509 term environmental forecasts. This could be done through an extension of our framework, by
510 including the relevant dynamic environmental covariates in the operating model (e.g., Thorson,
511 2019). If such distribution shifts are recent or ongoing it may be prudent to conduct the
512 optimization based on the predicted population densities in only the most recent years (e.g.,
513 Ault et al., 1999) .

514

515 Fisheries-independent surveys provide the foundation for scientifically sound fisheries
516 management, thus the design of those surveys should be optimized for multiple scientific
517 objectives. Using a heuristic approach, we designed a stratified survey design optimization that
518 meets the objectives of producing precise abundance indices with minimal sampling intensity for
519 multiple species. Major advantages of this approach are its explicit objectives of optimality and
520 maximal precision, flexibility of inputs and constraints, and ability to communicate the expected
521 impacts on the data products for downstream analyses. Systematically optimized survey designs
522 can quickly accommodate rapid modifications in sample size or species prioritization that often
523 arise as conditions change before or during a survey. The framework outlined here can be
524 modified to incorporate different operational constraints (e.g., total sample sizes, inaccessible
525 sampling units, and more detailed costs of sampling), species sets and species-specific precision
526 constraints, and data inputs. Given the prevalence of multispecies surveys in fisheries and
527 wildlife management among other applications, we hope that future survey design research will

528 use and extend this approach for multispecies survey optimization to better balance objectives
529 and further explore the tradeoffs inherent with surveying species with differing distributions of
530 abundance.

531

532 **Supplementary Material**

533 The following supplementary material is available at *ICESJMS* online. Supplementary Material 1
534 contains technical details for the operating model. Supplementary Material 2 is the predicted spatial
535 distributions for each species. Supplementary Material 3-10 contains additional result plots referred
536 to in the main text.

537

538 **Acknowledgements**

539 We thank all staff of the Alaska Fisheries Science Center's Groundfish Assessment Program
540 (GAP), program affiliates, volunteers, and charter captains and crew for collecting the data
541 analyzed here during the Gulf of Alaska Groundfish Bottom Trawl Survey. This research was
542 performed while ZSO held an NRC Research Associateship award at the NOAA Alaska
543 Fisheries Science Center. We also thank the Gulf of Alaska and Aleutian Islands Team within
544 GAP for their constructive feedback on earlier versions of this analysis. Finally, we thank James
545 Thorson, Dana Hanselman and two anonymous reviewers for comments that improved the
546 manuscript.

547

548 **Data Availability Statement**

549 The data and code underlying this article are available in the corresponding author's GitHub
550 account (https://github.com/zoyafuso-NOAA/Optimal_Allocation_GoA_Manuscript).

551

552
553
554
555
556
557
558
559
560
561
562
563
564
565
566
567
568
569
570
571
572
573

References

Ault, J. S., Diaz, G. A., Smith, S. G., Luo, J., and Serafy, J. E. 1999. An efficient sampling survey design to estimate pink shrimp population abundance in Biscayne Bay, Florida. *North American Journal of Fisheries Management*, 19: 696-712.

Ballin, M., and Barcaroli, G. 2013. Joint determination of optimal stratification and sample allocation using genetic algorithm. *Survey Methodology*, 39: 369-393.

Barbeaux, S., Aydin, K., Fissel, B., Holsman, K., Laurel, B., Palsson, W., Shotwell, K., Yang, Q., and Zador, S. 2018. Assessment of the Pacific cod stock in the Gulf of Alaska. In: *Stock assessment and fishery evaluation report for the groundfish resources of the Gulf of Alaska*. North Pacific Fishery Management Council.

Barcaroli, G. 2014. *SamplingStrata: An R package for the optimization of stratified sampling*. *Journal of Statistical Software*, 61: 1-24.

Bethel, J. 1989. Sample allocation in multivariate surveys. *Survey Methodology*, 15: 47-57.

Cao, J., Chen, Y., Chang, J. H., and Chen, X. 2014. An evaluation of an inshore bottom trawl survey design for American lobster (*Homarus americanus*) using computer simulations. *Journal of Northwest Atlantic Fishery Science*, 46: 27-39.

de Boois, I. J. (Ed). 2019. *Moving towards integrated ecosystem monitoring*. ICES Cooperative Research Report No. 347. 44 pp.

Field, S. A., Tyre, A. J., and Possingham, H. P. 2005. Optimizing allocation of monitoring effort under economic and observational constraints. *The Journal of Wildlife Management*, 69: 473-482.

574 Francis, R. I. C. C. 2006. Optimum allocation of stations to strata in trawl surveys. New Zealand
575 Fisheries Assessment Report, 23.

576 Francis, R. I. C. C. 2011. Data weighting in statistical fisheries stock assessment models.
577 Canadian Journal of Fisheries and Aquatic Sciences, 68: 1124-1138.

578 Hutniczak, B., Lipton, D., Wiedenmann, J., and Wilberg, M. 2019. Valuing changes in frequency
579 of fish stock assessments. Canadian Journal of Fisheries and Aquatic Sciences, 76: 1640-
580 1652.

581 ICES. 2020. ICES Workshop on unavoidable survey effort reduction (WKUSER). ICES
582 Scientific Reports, 2: 72. 92 pp.

583 Kotwicki, S., and Ono, K. 2019. The effect of random and density-dependent variation in
584 sampling efficiency on variance of abundance estimates from fishery surveys. Fish and
585 Fisheries, 20: 760-774.

586 Lanthier, G., Boisclair, D., Bourque, G., Legendre, P., Lapointe, M., and Angers, B. 2013.
587 Optimization of temporal versus spatial replication in the development of habitat use
588 models to explain among-reach variations of fish density estimates in rivers. Canadian
589 Journal of Fisheries and Aquatic Sciences, 70: 600-609.

590 Laurel, B. J., and Rogers, L. A. 2020. Loss of spawning habitat and prerecruits of Pacific cod
591 during a Gulf of Alaska heatwave. Canadian Journal of Fisheries and Aquatic Sciences,
592 77: 644-650.

593 Miller, T. J., Skalski, J. R., and Ianelli, J. N. 2006. Optimizing a stratified sampling design
594 when faced with multiple objectives. ICES Journal of Marine Science, 64: 97-109.

595 Mueter, F. J., and Norcross, B. L. 2002. Spatial and temporal patterns in the demersal fish
596 community on the shelf and upper slope regions of the Gulf of Alaska. *Fishery Bulletin*,
597 100: 559-581.

598 Muhling, B. A., Brodie, S., Smith, J. A., Tommasi, D., Gaitan, C. F., Hazen, E. L., Jacox, M. G.,
599 *et al.* 2020. Predictability of species distributions deteriorates under novel
600 environmental conditions in the California Current System. *Frontiers in Marine*
601 *Science*, 7.

602 Muradian, M. L., Branch, T. A., and Punt, A. E. 2019. A framework for assessing which
603 sampling programmes provide the best trade-off between accuracy and cost of data in
604 stock assessments. *ICES Journal of Marine Science*, 76: 2102-2113.

605 NMFS, 2020. Fisheries of the United States, 2018. U.S. Department of Commerce, NOAA
606 Current Fishery Statistics No. 2018. 167 pp.

607 Overholtz, W., Jech, J., Michaels, W., Jacobson, L., and Sullivan, P. 2006. Empirical
608 comparisons of survey designs in acoustic surveys of Gulf of Maine-Georges Bank
609 Atlantic herring. *Journal of Northwest Atlantic Fishery Science*, 36: 127-144.

610 Peel, D., Bravington, M., Kelly, N., Wood, S. N., and Knuckey, I. 2012. A model-based
611 approach to designing a fishery-independent survey. *Journal of Agricultural, Biological,*
612 *and Environmental Statistics*, 18: 1-21.

613 Regular, P. M., Robertson, G. J., Lewis, K. P., Babyn, J., Healey, B., and Mowbray, F. 2020.
614 SimSurvey: An R package for comparing the design and analysis of surveys by
615 simulating spatially-correlated populations. *PLoS One*, 15: e0232822.

616 Rhodes, J. R., and Jonzén, N. 2011. Monitoring temporal trends in spatially structured
617 populations: how should sampling effort be allocated between space and time?
618 *Ecography*, 34: 1040-1048.

619 Smith, S. G., Ault, J. S., Bohnsack, J. A., Harper, D. E., Luo, J., and McClellan, D. B. 2011.
620 Multispecies survey design for assessing reef-fish stocks, spatially explicit management
621 performance, and ecosystem condition. *Fisheries Research*, 109: 25-41.

622 Smith, S. J., and Hubley, B. 2013. Impact of survey design changes on stock assessment advice:
623 sea scallops. *ICES Journal of Marine Science*, 71: 320-327.

624 Thorson, J.T., 2019. Measuring the impact of oceanographic indices on species distribution
625 shifts: The spatially varying effect of cold-pool extent in the eastern Bering Sea.
626 *Limnology and Oceanography*, 64: 2632-2645.

627 Thorson, J. T., and Barnett, L. A. K. 2017. Comparing estimates of abundance trends and
628 distribution shifts using single- and multispecies models of fishes and biogenic habitat.
629 *ICES Journal of Marine Science*, 74: 1311-1321.

630 Thorson, J. T., Fonner, R., Haltuch, M. A., Ono, K., and Winker, H. 2017. Accounting for
631 spatiotemporal variation and fisher targeting when estimating abundance from
632 multispecies fishery data. *Canadian Journal of Fisheries and Aquatic Sciences*, 74: 1794-
633 1807.

634 Thorson, J. T., Shelton, A. O., Ward, E. J., and Skaug, H. J. 2015. Geostatistical delta-
635 generalized linear mixed models improve precision for estimated abundance indices for
636 West Coast groundfishes. *ICES Journal of Marine Science*, 72: 1297-1310.

637 v on Szalay, P.G. 2015. The impact of sample size reduction on the precision of biomass
638 estimates in the Gulf of Alaska. U.S. Department of Commerce, NOAA Technical
639 Memorandum NMFS-AFSC-297. 17 pp.

640 v on Szalay, P. G., and Raring, N. W. 2018. Data report: 2017 Gulf of Alaska bottom trawl
641 survey. U.S. Department of Commerce, NOAA Technical Memorandum NMFS-AFSC-
642 374. 260 pp.

643 v on Szalay, P. G., Raring, N. W., Shaw, F. R., Wilkins, M. E., and Martin, M. H. 2010. Data
644 report: 2009 Gulf of Alaska bottom trawl survey. U.S. Department of Commerce, NOAA
645 Technical Memorandum NMFS-AFSC-208. 245 p.

646 Wang, J., Xu, B., Zhang, C., Xue, Y., Chen, Y., and Ren, Y. 2018. Evaluation of alternative
647 stratifications for a stratified random fishery-independent survey. *Fisheries Research*,
648 207: 150-159.

649 Xu, B., Ren, Y., Chen, Y., Xue, Y., Zhang, C., and Wan, R., 2015. Optimization of stratification
650 scheme for a fishery-independent survey with multiple objectives. *Acta Oceanologica*
651 *Sinica*, 34: 154-169.

652 Zador, S., Yasumiishi, E., and Whitehouse, G. A. 2019. Ecosystem Status Report 2019 Gulf of
653 Alaska. North Pacific Fishery Management Council. 232 pp.

654 Zimmermann, F., and Enberg, K., 2016. Can less be more? Effects of reduced frequency of
655 surveys and stock assessments. *ICES Journal of Marine Science*, 74; 56-68.

656

657

658

659

660

661

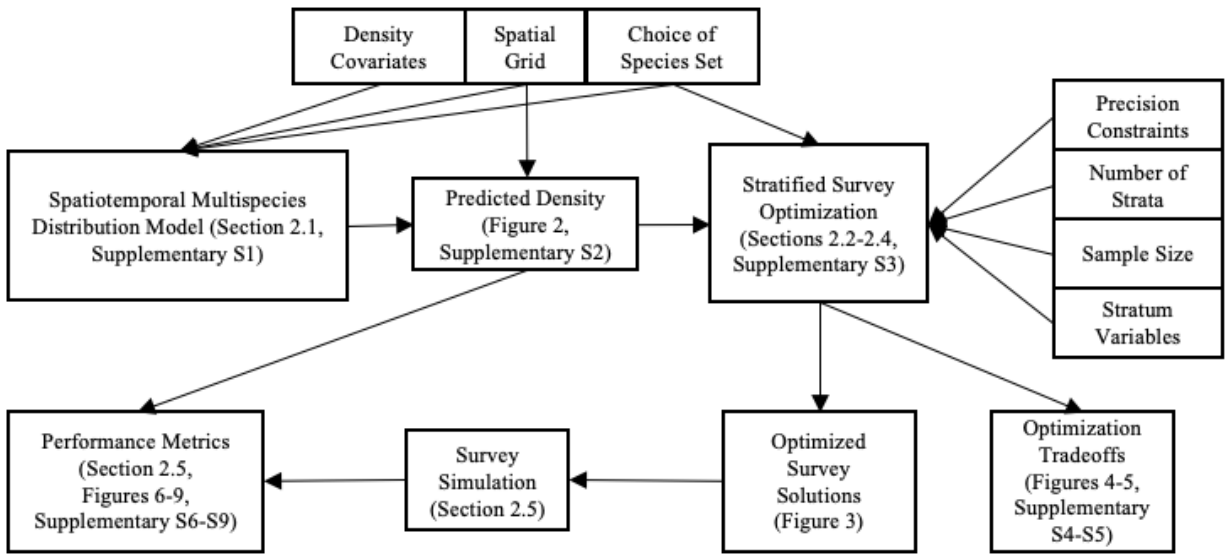
662

663

664

665

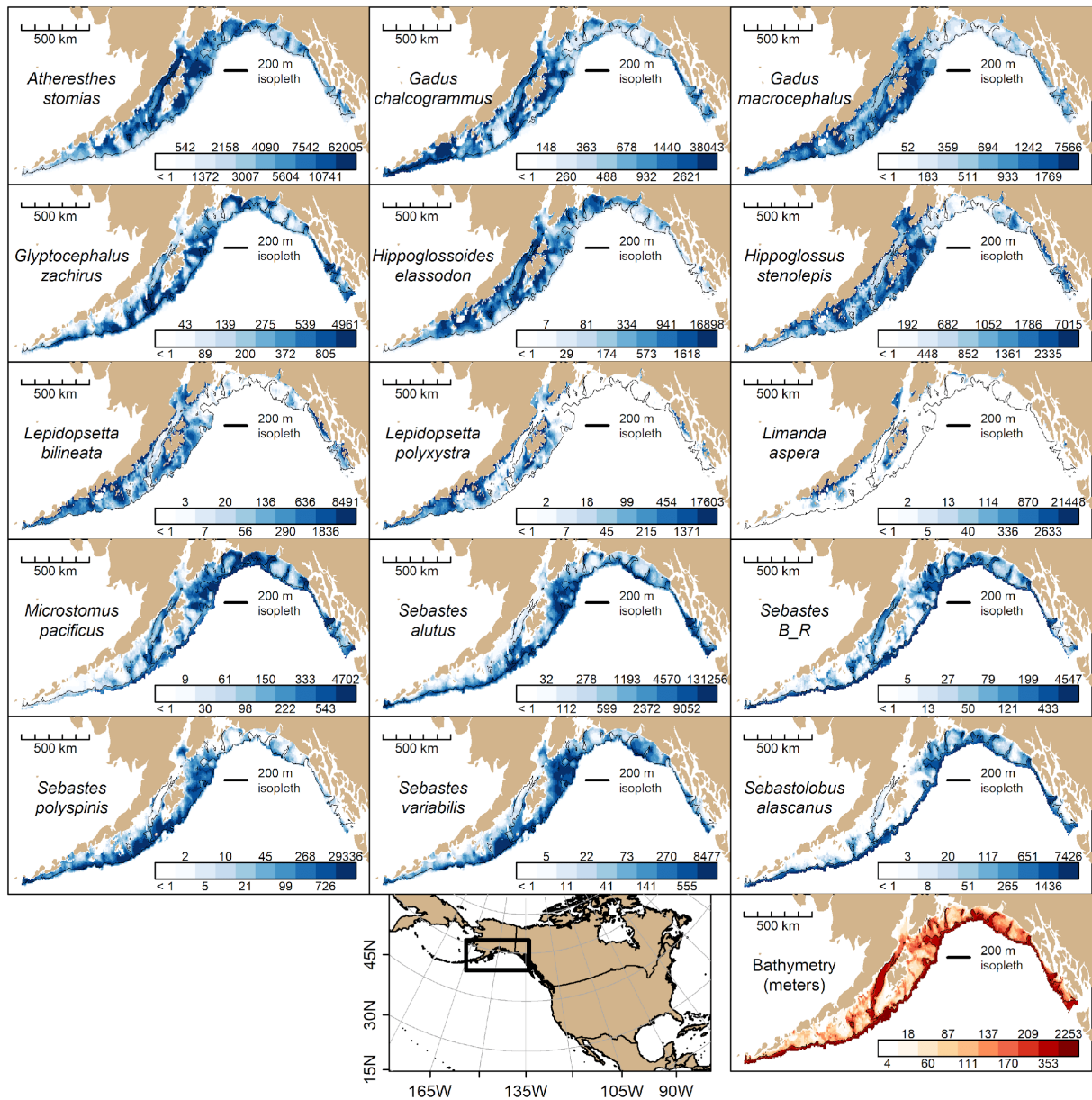
666 **Figures**



667

668 Figure 1: Flowchart of the multispecies stratified survey optimization.

669



670

671 Figure 2: Predicted mean density across years (kg km^{-2}) for each species included in the survey

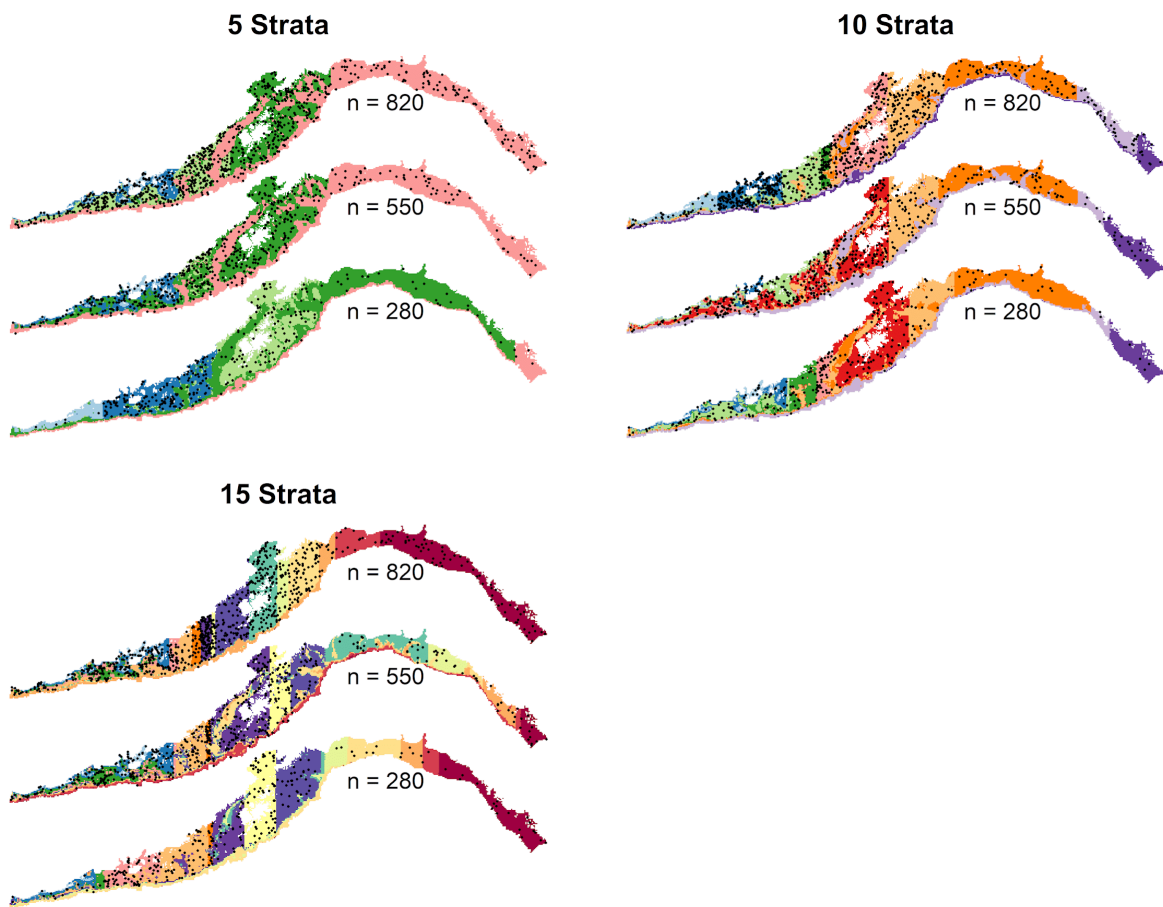
672 optimization across the Gulf of Alaska. Bottom right panel shows the bathymetry within the

673 survey footprint along with the 200 m isobath, which is a general delineation of species

674 distributions. Refer to the Supplementary S1 for a brief explanation of the operating model used

675 to produce these predicted densities and Supplementary S2 for predicted densities by year.

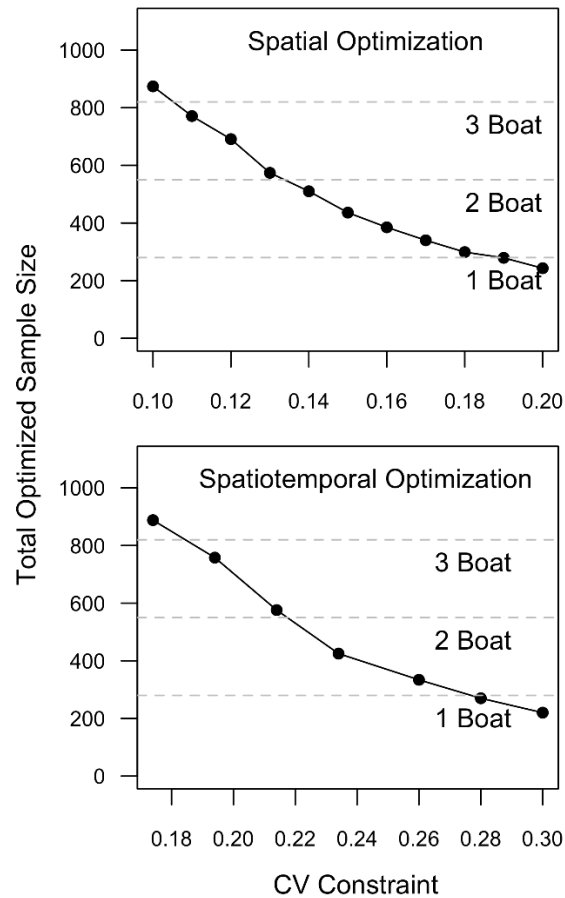
676



677

678 Figure 3: Representative examples of strata boundary maps arising from solutions for the
 679 species-specific CV constraint optimization for five, ten, and fifteen strata across the three effort
 680 (boats) scenarios with simulated stations randomly sampled according to each optimized
 681 stratified survey superimposed. The colors represent different strata .

682



683

684 Figure 4: Total optimized sample size (number of stations) across coefficient of variation

685 (CV) constraint, accounting only for spatial variability (top) or both spatial and temporal

686 variability (bottom). The five-strata optimization solutions are shown, but qualitative results

687 were consistent across strata (Supplementary S4). Both optimizations were conducted under

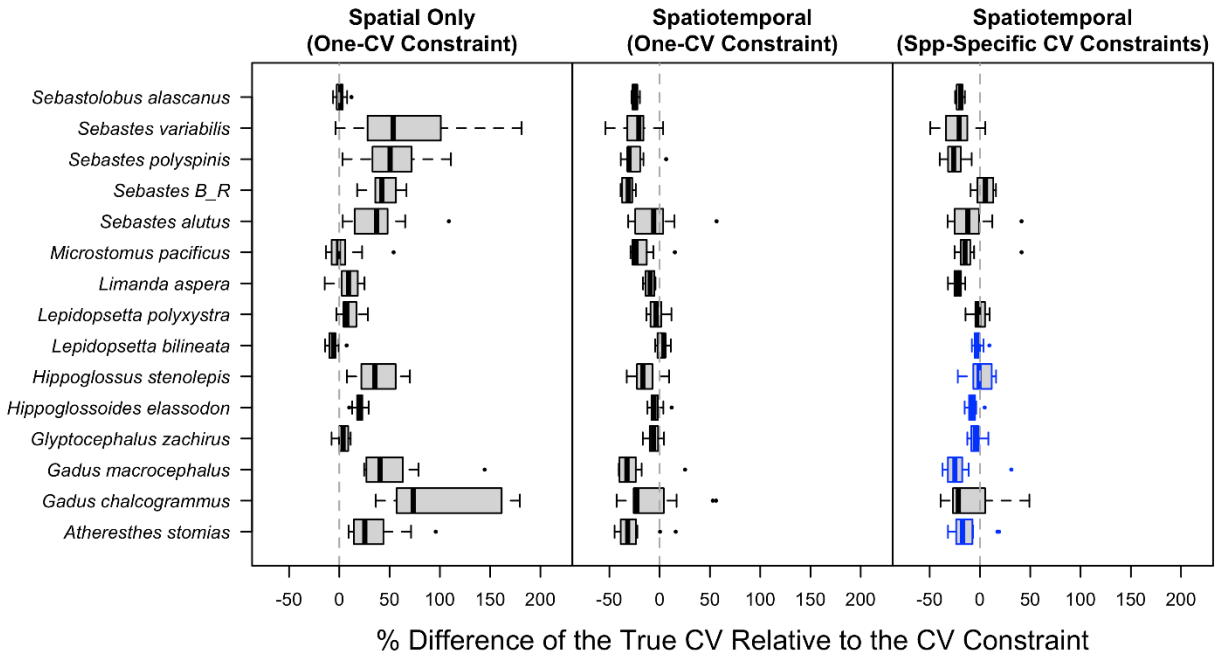
688 the one-CV constraint approach where all species have the same CV constraint in the

689 optimization. Horizontal dotted grey lines indicate the sampling levels for one, two, and three

690 boat-effort scenarios .

691

692



693 % Difference of the True CV Relative to the CV Constraint

694 Figure 5: Comparison of the relative difference between expected and realized coefficient of

695 variation (CV) of abundance. Specifically, this shows the distribution of percent differences of

696 the true CVs, calculated for each year, relative to the CV constraint associated with a five-

697 strata, two boat -effort scenario (n = 550) for all included species. The left and center plots

698 show optimizations using the one-CV constraint approach. The right plot shows an optimization

699 using the species-specific CV constraint approach (refer to the main text for how CV constraints

700 were specified across species). For the species-specific CV constraint approach, a value of 0.10

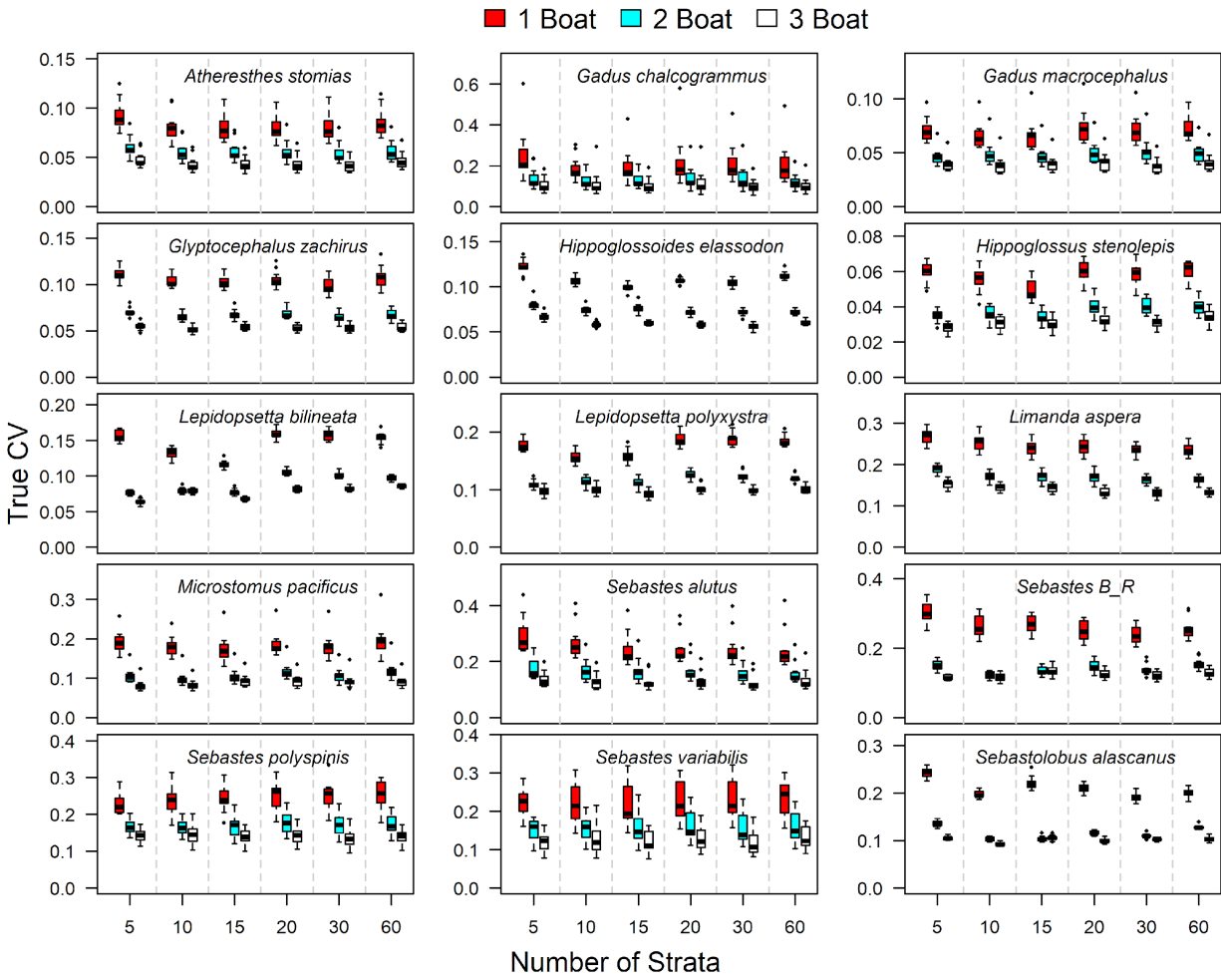
701 was chosen as the lowest a population CV constraint could be specified (indicated by the blue

702 borders). A positive value indicates that the observed true CV is greater than the CV

703 constraint that was specified in the optimization. A negative or near-zero value

704 indicates that the observed true CV is within the CV constraint specified in the

705 optimization. Results were qualitatively consistent with other total effort and strata scenarios.



707

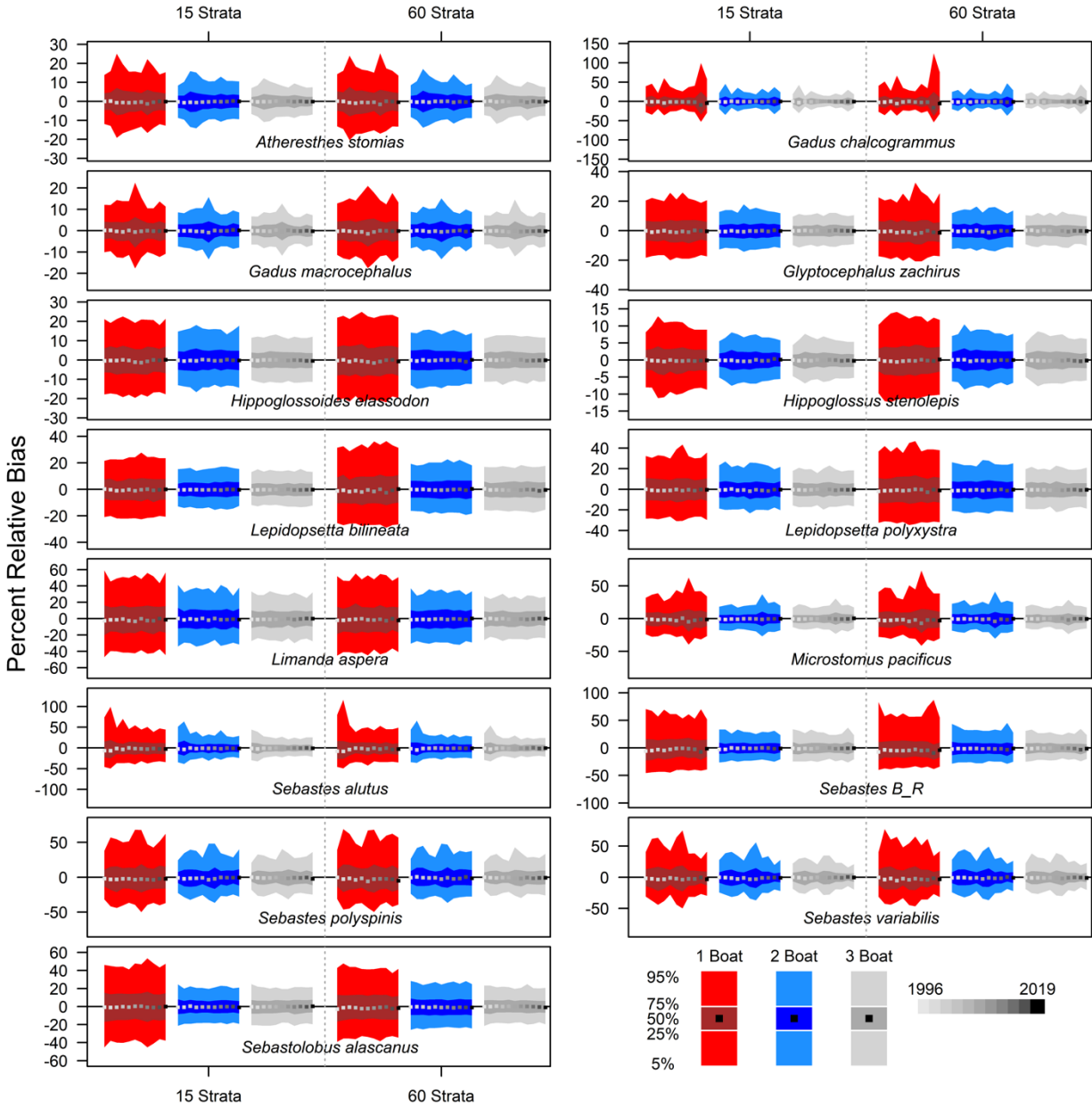
708 Figure 6: Distribution of true coefficient of variation (CV) across observed years for each

709 species, level of sampling effort (color) and number of strata for the species-specific CV

710 constraint approach.

711

712



713

714 Figure 7: Distribution of percent relative bias in the simulated mean density estimates across

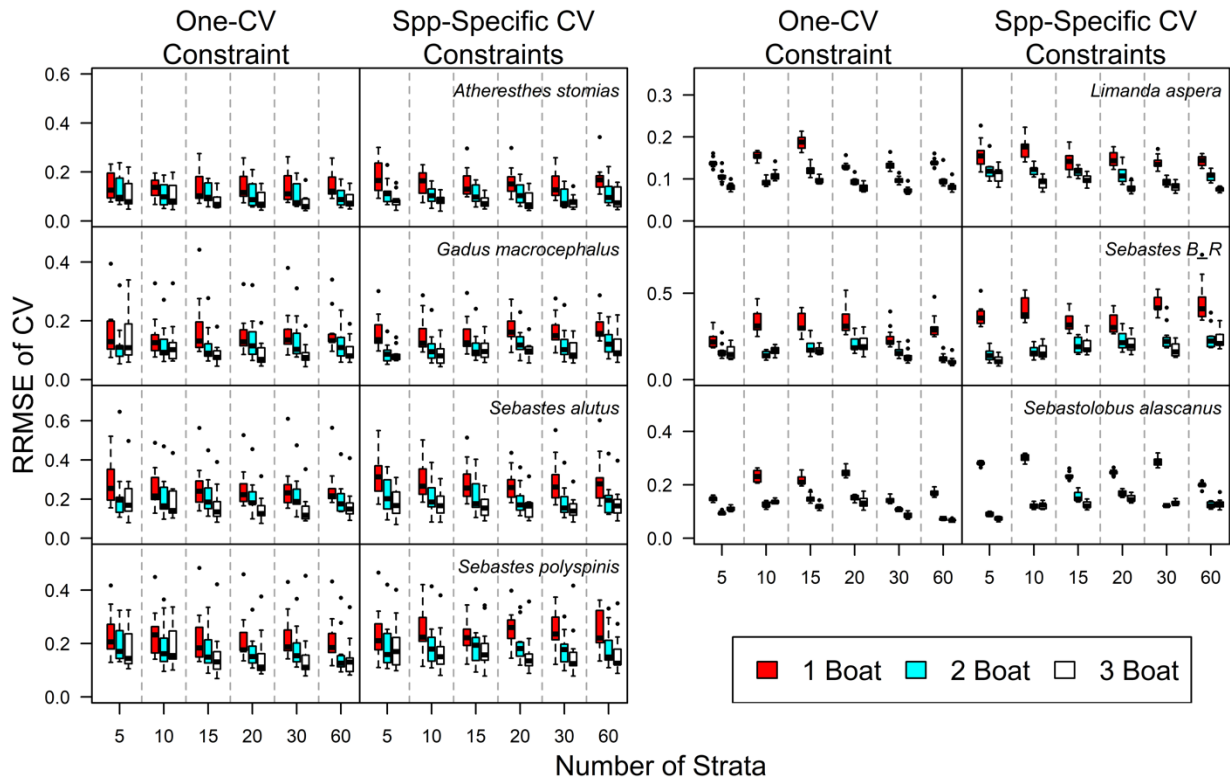
715 years relative the true mean density for each species, level of sampling effort (color) and

716 two strata levels (15 and 60 to represent the range investigated) for the species-specific CV

717 constraint approach. Results were similar for the one-CV constraint approach (Supplementary

718 S8).

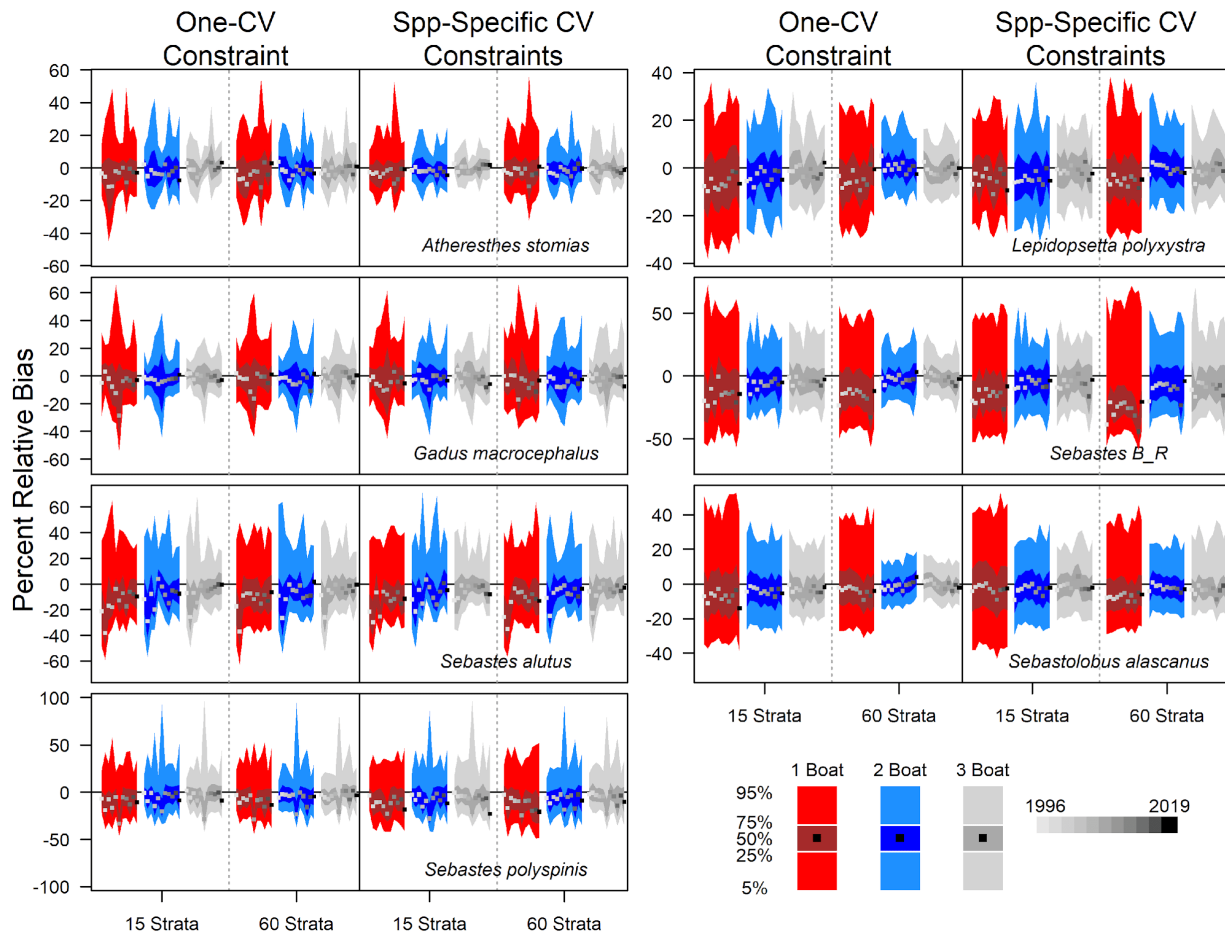
719



721

722 Figure 8: Distribution of relative root mean square error (RRMSE) of the coefficient of variation
 723 (CV) across observed years for a subset of species (see Supplementary S7 for a full version),
 724 level of sampling effort (color) and number of strata for the one-CV constraint approach (left set
 725 of plots) and species-specific CV constraint approach (right set of plots) .

726



728

729 Figure 9: Distribution of percent relative bias in the simulated coefficient of variation (CV)
 730 estimates across observed years relative the true CV for a subset of species (see
 731 Supplementary S9-10 for a full version), level of sampling effort (color) and two strata levels (15
 732 and 60 to represent the range investigated) for the species-specific CV constraint approach.
 733